Quantum Yield of Formaldehyde Formation in the Presence of Colloidal TiO_2-Based Photocatalysts: Effect of Intermittent Illumination, Platinization, and Deoxygenation

Chuan-yi Wang,*,† Ronald Pagel,‡ Detlef W. Bahnemann,*,§ and Jürgen K. Dohrmann‡

Chemistry Department, Tufts University, 62 Talbot Avenue, Medford, Massachusetts 02155, Institut für Chemie/Physikalische und Theoretische Chemie, Freie Universität Berlin, Takustrasse 3, D-14195 Berlin, Germany, and Institut für Technische Chemie, Universität Hannover, Callinstrasse 3, D-30167 Hannover, Germany

Received: May 6, 2004; In Final Form: July 2, 2004

Colloidal TiO_2 (2.4 nm average particle diameter) has been prepared and modified by photodeposition of Pt (PtTi-S1) and by mixing with Pt nanoparticles (PtTi-S2). Transmission electron microscopy reveals particle aggregation in colloidal TiO_2 and large networks of agglomerated particles in the platinized samples. The photocatalytic activity of the samples (0.1 g L^{-1}) has been investigated by measuring the quantum yield, ϕ_{HCHO}, of HCHO formed from aqueous methanol at pH 3.5 under different conditions. In CW photolysis of the oxygenated suspensions (300−400 nm UV light, 8×10^{-7} einstein L^{-1} s^{-1} photon absorption rate) the platinized photocatalysts (1 wt % Pt) enhance ϕ_{HCHO} by a factor of 1.5−1.7 with respect to neat colloidal TiO_2 where ϕ_{HCHO} is 0.02. In addition to the action of Pt as an electron sink, the strong promotion of photocatalytic methanol oxidation by PtTi-S2 at the small Pt/TiO_2 particle ratio of ca. 1:1060 is proposed to arise from transfer of excitation energy or of photogenerated charge carriers through the particle network. Repetitive laser-pulse illumination of the oxygenated samples (351 nm, 0.5 Hz repetition frequency) increases ϕ_{HCHO} by ca. 50% in comparison with CW illumination at the same average photon absorption rate of ca. 8×10^{-7} einstein L^{-1} s^{-1}. As a tentative explanation an increase of the photocatalyst surface by laser-pulse stimulated deaggregation of colloidal TiO_2 and fragmentation of the networks in the platinized samples is suggested. HCHO is also produced in the deoxygenated suspensions under repetitive laser-pulse illumination. PtTi-S1 and PtTi-S2 increase ϕ_{HCHO} by factors of 1.8 and 1.2, respectively, in comparison with neat colloidal TiO_2 where ϕ_{HCHO} is 0.027. Possible mechanisms are discussed. The higher activity of PtTi-S1 is attributed to stronger electrocatalysis of H_2 formation by highly dispersed Pt in PtTi-S1 as compared with the Pt particles in PtTi-S2.

1. Introduction

Photocatalysis using semiconductor particles, with a primary focus on titanium dioxide, TiO_2, has found increasing interest to solve a wide variety of problems concerning environmental pollution.[1−13] The primary events responsible for the photoinitiated catalytic or synthetic reactions are interfacial redox processes of light-generated electrons and holes. Although the detailed mechanisms of photocatalysis vary with different reactants, it appears that hydroxyl-type radical intermediates produced by the reaction of photogenerated holes with hydroxide ions or water molecules adsorbed on TiO_2 play a vital role in the photodegradation of organic pollutants.[1,2,5−7,10,11]

Sun and Bolton studied the photocatalytic formation of formaldehyde (HCHO) from methanol in oxygenated aqueous suspensions of TiO_2 (anatase) particles and derived the quantum yield of the OH radical considered as the oxidizing intermediate.[14] We used the same oxidation reaction in order to investigate the activity of different types of titanium dioxide photocatalysts (colloidal TiO_2 particles of nominally 2.4 nm diameter, Degussa P 25, Sachtleben Hombikat UV 100) by the measurement of the HCHO quantum yield, ϕ_{HCHO}, after continuous UV photolysis of their aqueous suspensions containing methanol.[15,16] Several factors, such as catalyst loading, pH, and photon flux, important for the photocatalytic activity were studied. The low value of ϕ_{HCHO} on neat colloidal TiO_2 (0.02 at 8×10^{-7} einstein L^{-1} s^{-1} photon absorption rate) demonstrated again the main bottleneck to the application of semiconductor photocatalysis for large-scale water treatment.[10]

The present work is an extension of our efforts to improve the photocatalytic activity of colloidal TiO_2 particles[17,18] and to consider the consequences of the previously discovered network structure of these particles[18,19] for the efficiency of photocatalytic methanol oxidation. Apart from the favorable effect of doping the TiO_2 particles with Fe(III) ions,[17,18,20] the presence of platinum as an electron sink has long been known to enhance the separation of photogenerated electron−hole pairs[21] and, hence, to improve the photocatalytic efficiency in general.[22−26] However, most of the previous studies were focused on the influence of the extent of platinization.

In the present paper we report on the preparation and characterization, e.g., by transmission electron microscopy (TEM), of two types of $Pt@TiO_2$ photocatalysts which both improved the HCHO quantum yield by at least 50% in comparison with neat colloidal TiO_2 particles at a platinum

* To whom correspondence should be addressed. E-mail: chuanyi.wang@tufts.edu (C.-y.W.); bahnemann@iftc.uni-hannover.de (D.W.B.).
† Tufts University.
‡ Freie Universität Berlin.
§ Universität Hannover.

10.1021/jp048046s CCC: $27.50
Published on Web 08/21/2004

SCHEME 1: Setup for Repetitive 351 nm Laser-Pulse Photolysis

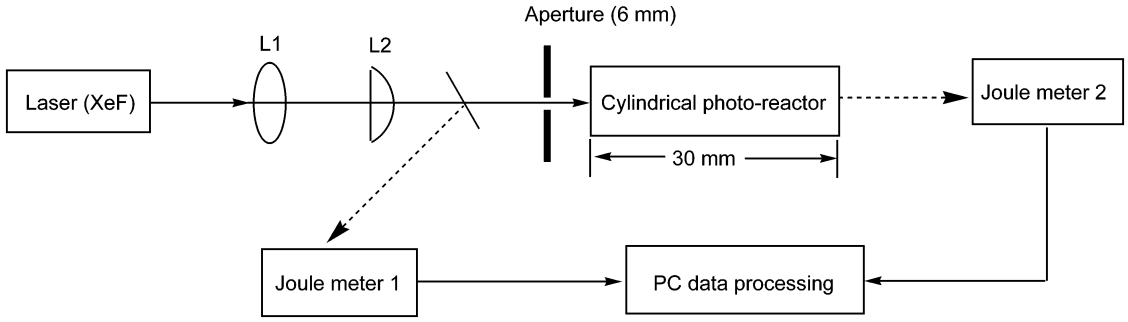

content as low as 1 wt %. The Pt@TiO_2 samples were prepared by photochemical platinization of colloidal TiO_2 and by mixing of colloidal Pt and TiO_2. The improvement of ϕ_{HCHO} was found in continuous (CW) UV photolysis and after repetitive 351 nm laser-pulse photolysis of the oxygenated aqueous suspensions of the Pt@TiO_2 photocatalysts.

Another point of recent interest in TiO_2 photocatalysis is the effect of intermittent illumination on the efficiency.[27−32] For example, a study by Cornu et al. indicated that quantum yields of formate oxidation in aqueous TiO_2 suspensions measured under variable-frequency periodic illumination were always *smaller* than, but approached, at sufficiently rapid intermittence, the quantum yields measured under continuous exposure at equivalent average photon absorption rates.[32]

Here, we report also on the effects of repetitive 351 nm laser-pulse illumination (ca. 20 ns to 2 s light-to-dark ratio) on the quantum yield of formaldehyde formation, ϕ_{HCHO}, measured in aqueous methanolic suspensions of neat colloidal TiO_2 and the above Pt@TiO_2 photocatalysts both in the presence and absence of oxygen. Experimental conditions were chosen to ensure that the methanol conversion within any single experiment never exceeded 1% ensuring that the photocatalytic process could always be studied without any mass-transport limitations. For a given photocatalyst, repetitive illumination resulted in an up to ca. 50% increase of ϕ_{HCHO} with respect to CW illumination; however, differences in the increase were seen depending on the presence or absence of oxygen. We attribute the observed increase of ϕ_{HCHO} to the laser-pulse-induced deaggregation of the TiO_2-particle networks seen here and previously in the TEM images. Models for this effect as well as for the mechanisms of photocatalytic methanol oxidation on the above catalysts in the presence or absence of oxygen will be discussed.

2. Experimental Section

2.1. Materials. Chemicals including $TiCl_4$ (Merck-Schuchardt), CH_3OH (Merck), 2,4-dinitrophenylhydrazine (DNPH, Aldrich), $Na_2HPO_4 \cdot 12H_2O$ (Merck), etc. were commercial products and used as received without further purification. Water was purified by a Milli-Q/RO system (Millipore) and had a resistivity ≥ 18 MΩ cm.

2.2. Preparation of Samples. Colloidal TiO_2 was prepared as reported elsewhere.[17,33,34] In brief, 2.8 mL of $TiCl_4$ prechilled to −20 °C was added slowly to 800 mL of stirred water at 0 °C. After being continuously stirred for 40 min at the same temperature, the reaction solution was dialyzed against water using a membrane (Medicell International Ltd., London, U.K. size 9, Inf Dia 36/32, molecular weight cutoff 12−14 000 daltons) at room temperature to change the pH from 1.7 to 2.35. Following rotary evaporation of the as-above-prepared colloidal solutions at room temperature under vacuum, white or slightly yellowish shining crystal-like powders were obtained. As-prepared TiO_2 has the structure of anatase. The average particle diameter is ca. 2.4 nm as determined by transmission electron microscopy.

The Pt@TiO_2 photocatalysts were prepared by the following two methods.

2.2.1. Method 1: Photochemical Deposition of Platinum. H_2PtCl_6 was added to aqueous colloidal TiO_2 solutions in the desired ratio. Then, the solution was illuminated with UV-A light for 1.5 h. Evaporation of the resulting solution under vacuum at room temperature yielded a brownish powder sample.

2.2.2. Method 2: Mixing of Colloidal Platinum and Titanium Dioxide. Colloidal Pt (particle diameters ca. 3 nm) was prepared by reduction of H_2PtCl_6 with sodium citrate.[21] Excess ions in the resulting colloidal suspension were removed with an ion-exchange resin until a specific conductivity of ca. 3 μS cm^{-1} was reached. As-prepared colloidal Pt was then mixed with colloidal TiO_2 in the desired ratio. After evaporation under vacuum at room temperature, a brownish powder was obtained.

The Pt@TiO_2 samples could be resuspended in water, methanol, and in the mixture of both solvents and yielded transparent colloidal suspensions. The photocatalysts prepared by the methods 1 and 2 are denoted as PtTi-S1 and PtTi-S2, respectively, hereafter.

2.3. TEM/HRTEM. Size, shape, and crystal structure of the sample photocatalysts were characterized by different transmission electron microscopic (TEM) techniques. All investigations were carried out with a Philips Tecnai F20 (FEI Company, Oregon) equipped with a field emission gun operating at 160 kV. TEM samples were prepared by placing droplets of the aqueous suspension of the nanoparticles on carbon-covered copper grids for 30 s. Subsequently, the supernatant fluid was blotted off and the grids were dried in air. For quantitative evaluations, all nominal values of magnification and camera length were corrected by the use of a gold calibration standard (W. Plannet, Wetzlar, Germany).

2.4. Photolysis. CW photolyses were carried out as detailed previously.[15,16] CW light was provided by a Xe lamp. The wavelength selection was achieved by a set of band-pass filters (Black and WG 320, photoactive wavelengths, 300−400 nm).

For intermittent photolysis at 351 nm, pulses (width 10−20 ns) from a XeF excimer laser were applied at a repetition frequency of 0.5 Hz. Laser-pulse photolyses were carried out in a 3 mL cylindrical cell equipped with optical grade quartz windows (Scheme 1). The optical path length of the cylindrical photolysis zone (0.6 cm diameter) was 3 cm. The absorbed light energy was determined by use of two joulemeters (Gentec ED-200 and ED-500) in conjunction with spectrophotometry. The joulemeters were calibrated actinometrically (Aberchrome 540[35]). Actinometry was performed in the cell used for laser photolysis in order to avoid corrections for light reflection and cell

geometry. Because of the variation in laser-pulse energy, the meter readings were stored in a personal computer (Scheme 1).

Prior to repetitive laser-pulse photolysis, the aqueous suspension of the photocatalyst was saturated with oxygen. Thereafter, methanol was added, and the inlet of the cell was sealed to avoid leakage of oxygen during the photolysis. For studies under the exclusion of oxygen, the solution was thoroughly flushed with N_2 prior to the addition of methanol, and the cell was again kept sealed during the photolysis.

All the photolyses were carried out at room temperature in aqueous photocatalyst suspensions containing methanol at pH 3.5. As an appropriate quantity for comparing the conditions applied for CW and repetitive laser-pulse photolysis, the time-average of the absorbed photon flux, $\langle I_a \rangle$, in units of einstein L^{-1} s^{-1} was considered.

The activity of the photocatalysts under different conditions of photolysis was assessed by the determination of the quantum yield, ϕ, of HCHO formation by photooxidation of methanol. ϕ is defined as

$$\phi = R/I_a \tag{1}$$

where

$$I_a = I_0 F_s \tag{2}$$

R is the photochemical formation rate of HCHO. I_a and I_0 are the absorbed and incident photon fluxes, respectively, in units of einstein L^{-1} s^{-1}. In CW photolysis, F_s is the integrated absorption fraction of the sample over the wavelength range used

$$F_s = \frac{\int_{\lambda_1}^{\lambda_2} I_\lambda T_\lambda^f f_\lambda^s \, d\lambda}{\int_{\lambda_1}^{\lambda_2} I_\lambda T_\lambda^f \, d\lambda} \tag{3}$$

I_λ is the relative incident photon flux in the wavelength band $d\lambda$, T_λ^f is the transmittance of the filter used in the experiment, and

$$f_\lambda^s = 1 - T_\lambda^s = 1 - 10^{-A_\lambda^s} \tag{4}$$

is the fraction of light absorbed at wavelength λ. T_λ^s and A_λ^s are the transmittance and absorbance, respectively, of the sample at wavelength λ. I_0 and F_s were determined by chemical actinometry[35] and spectrophotometry. In monochromatic laser photolysis, F_s is identical with f_λ^s, eq 4.

2.5. Analysis. The amount of HCHO formed by photooxidation of methanol was determined by HPLC after reacting HCHO with 2,4-dinitrophenylhydrazine (DNPH). As a standard reference, FA-DNPH (FA, formaldehyde) hydrazone was synthesized by the method described by Shriner et al.[36] The product was characterized by spectrophotometry[37] (see Figure 1, ϵ_{max} ca. 2.0×10^4 L mol^{-1} cm^{-1}), melting point[38] (165 °C), and chemical element composition analysis (theoretical: C/H/N/O = 40/2.86/26.67/30.47; experimental: C/H/N/O = 40.08/2.88/26.18/30.86). The purity of the product was checked by HPLC.

HPLC employed a Dionex 4500i chromatograph equipped with a 250 mm reversed-phase column (Nucleosil-100-10C18, 4 mm ID, Macherei-Nagel, Germany). The injection volume was 20 μL. The eluent consisted of CH_3OH, H_2O, and CH_3-COOH (60:40:0.5), and its flow rate was 1.5 mL/min. The absorbance detector was set at 360 nm.

The optical absorption of FA-DNPH, colloidal TiO_2, and Pt@TiO_2 was measured with a Perkin-Elmer Lambda 9 spectrophotometer equipped with an integrating sphere. The error of the measured absorbance was within ± 0.006. The relative error of the quantum yield of HCHO formation was $\leq \pm 0.002$ as judged from repeated runs under identical conditions of photolysis.

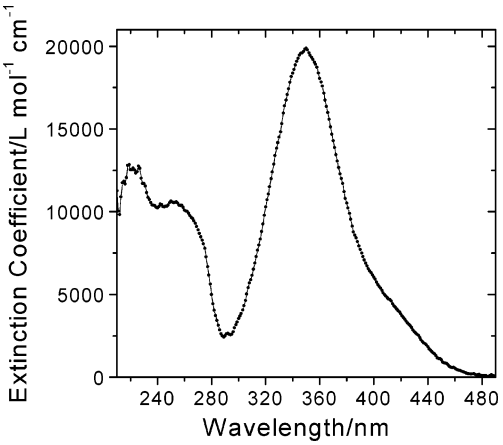

Figure 1. UV-vis spectrum of formaldehyde-(2,4)-dinitrophenylhydrazone in acetonitrile.

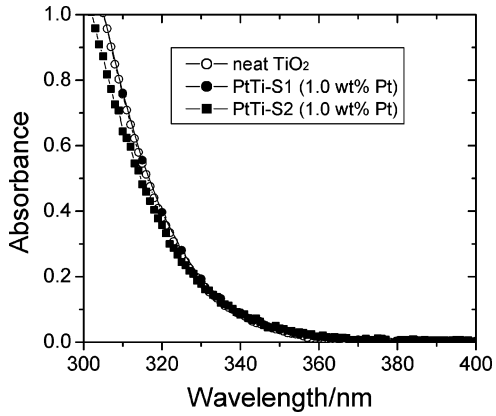

Figure 2. Absorption spectra of the colloidal TiO_2-based photocatalysts in aqueous suspensions (pH 3.5) at room temperature (0.1 g L^{-1} loading, 1 cm optical length). PtTi-S1: platinization by photodeposition. PtTi-S2: platinization by mixing of colloidal Pt and TiO_2.

3. Results

3.1. UV−Vis Spectra and Electron Microscopy. Figure 2 shows the absorption spectra of neat colloidal TiO_2 and of the platinized TiO_2 samples, PtTi-S1 and PtTi-S2, in aqueous suspensions. The optical absorption of TiO_2 appears only in the UV region, where the absorbance increases steeply below 360 nm as it is characteristic of TiO_2. There is virtually no light scattering at longer wavelength. Comparison of the spectra shown in Figure 2 evinces that the optical absorption of colloidal TiO_2 hardly changes when the particles are modified either by deposition of traces of platinum (PtTi-S1) or by mixing with colloidal platinum (PtTi-S2).

Figure 3 shows TEM pictures of the three photocatalysts, neat TiO_2, PtTi-S1 and PtTi-S2. The colloidal particles, which appear as globular or polyhedral objects, adhere to each other to form networks of different architectures. Neat colloidal TiO_2 (average particle diameter ca. 2.4 nm, see also ref 33) tends to form comparatively small aggregates with no distinct orientation. The Pt@TiO_2 samples clearly exhibit large networks of interconnected chains or branches of aggregated particles.

More detailed structural information is obtained from high-resolution (HR) TEM (Figure 4). In the HRTEM images crystal

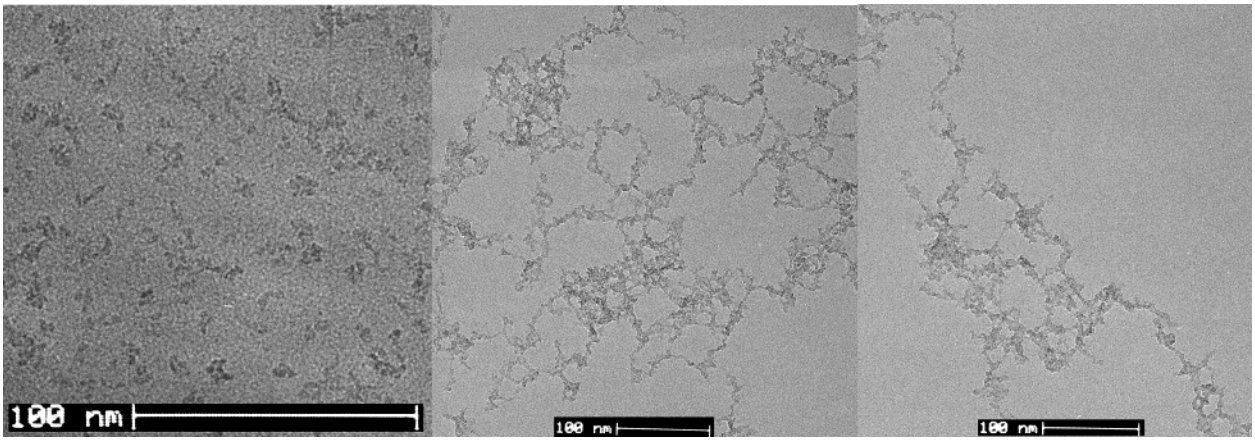

Figure 3. Transmission electron micrographs (TEM) of the photocatalysts: neat TiO_2 (nominal average particle diameter ca. 2.4 nm), PtTi-S1, and PtTi-S2 with 1 wt % Pt (from left to right).

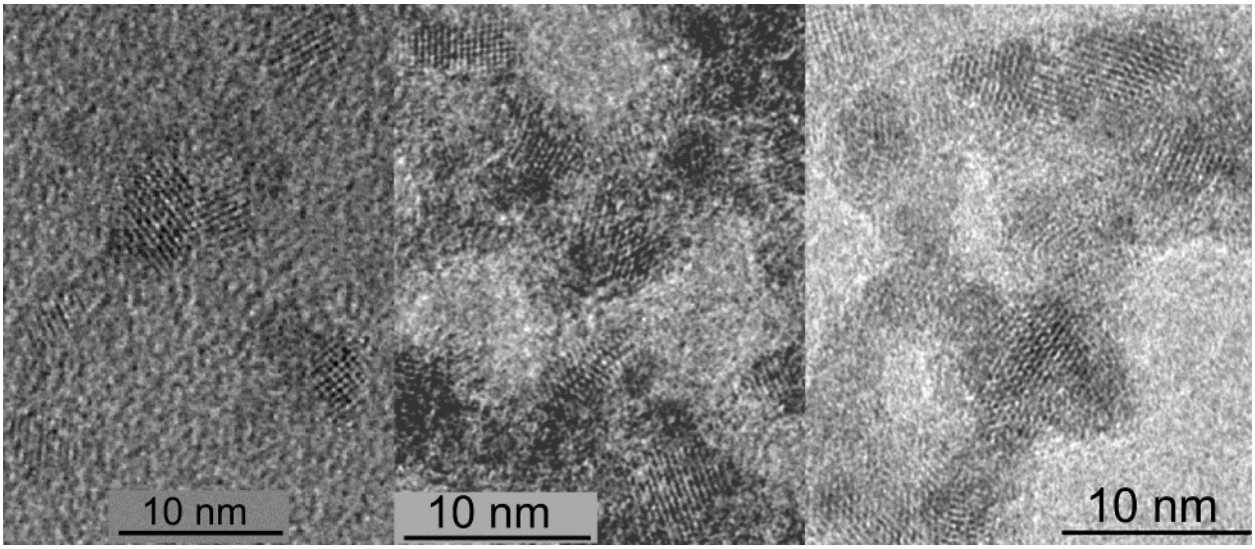

Figure 4. High-resolution transmission electron micrographs (HRTEM) of the neat TiO_2, PtTi-S1, and PtTi-S2 with 1 wt % Pt (from left to right).

planes of the particles compatible with the anatase modification of TiO_2 can be recognized. This was further confirmed by electron diffractograms and evaluations of the Fourier transforms of the HRTEM images (see also refs 18 and 19). No crystal structure corresponding to platinum was observed. This is understandable when considering the very small content of only 1 wt % Pt. As estimated from Figures 3 and 4, the size of the PtTi-S1 and PtTi-S2 particles falls in the range of 1.5−4 nm, comparable to that of neat TiO_2 particles which have an average diameter of ca. 2.4 nm.

3.2. Continuous Photolysis. The photocatalytic activity of colloidal TiO_2, PtTi-S1, and PtTi-S2 was investigated by the measurement of the quantum yield, ϕ_{HCHO}, of HCHO formed by photocatalytic oxidation of methanol. Upon exposure of O_2-saturated aqueous suspensions, containing one of the photocatalysts and methanol, to 300−400 nm CW light, HCHO was produced and identified quantitatively by HPLC analysis (section 2.5). Other products were not detected by HPLC. HCHO was not formed in the dark or during photolysis in the absence of the TiO_2-based samples, evincing that the process is truly photocatalytic.

Figure 5 demonstrates that the concentration of HCHO in the presence of the photocatalysts increases linearly with illumination time. Hence, the photochemical reaction rate is given by the slope of the straight lines shown in Figure 5. (The point for neat TiO_2 at 10 min irradiation time falls below the respective straight line. This deviation vanishes, when pre-irradiation of the aqueous photocatalyst is applied in the absence of CH_3OH.[17])

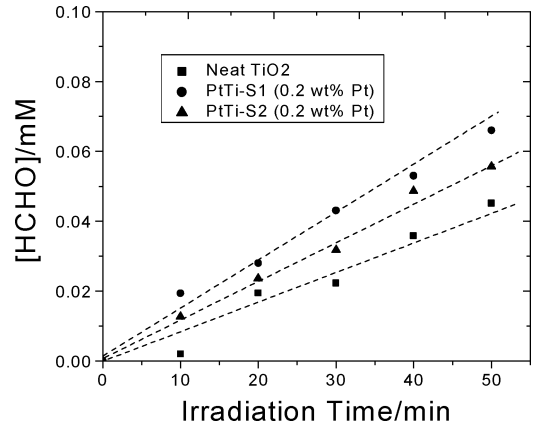

Figure 5. Production of HCHO in the presence of colloidal photocatalysts TiO_2, PtTi-S1 and PtTi-S2 as a function of illumination time during CW-photolysis. Catalyst loading, 100 mg/L; 30 mM aqueous CH_3OH (O_2-sat'd, pH 3.5); reaction volume, 50 mL; $I_0 = 3.37 \times 10^{-6}$ Einstein L^{-1} s^{-1} (ca. 300−400 nm). For catalyst preparation, see section 2.2.

By use of eqs 1−4, the quantum yields, ϕ_{HCHO}, in the presence of the various photocatalysts are readily obtainable. The result is shown in Figure 6 for neat colloidal TiO_2 and the Pt@TiO_2 catalysts at an increasing loading by platinum. Obviously,

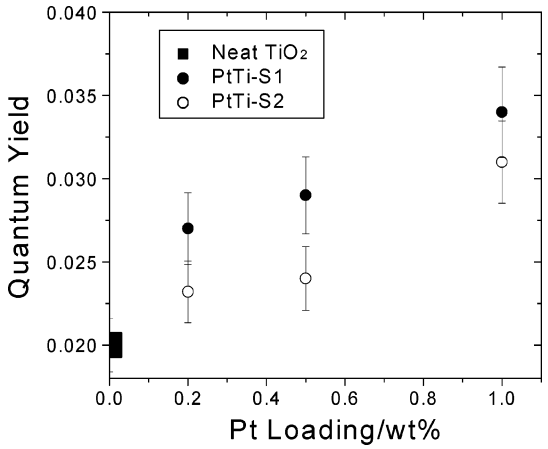

Figure 6. Quantum yields of photocatalytic formaldehyde formation from methanol in the presence of PtTi-S1 and PtTi-S2 as a function of Pt loading. For comparison: neat colloidal TiO_2. For conditions of photolysis, see Figure 5. ($F_s = 0.24$ derived from eq 3 in the wavelength range of 300−400 nm).

platinization has a strong promoting effect on the formation of HCHO in TiO_2-based photocatalysis. ϕ_{HCHO} increases by up to 50−70% when compared with that value on neat TiO_2 particles. From Figures 5 and 6, it is also seen that photochemical platinization of the TiO_2 particles yields a more efficient photocatalyst (PtTi-S1) than mixing of the colloidal components of Pt and TiO_2 (PtTi-S2).

3.3. Laser-Pulse Photolysis and Deoxygenation. Photocatalytic oxidation of aqueous methanol was also studied by applying repetitive 351 nm laser-pulse photolysis both in the presence and absence of oxygen as an electron acceptor (see Scheme 1 for the setup).

Table 1 lists the various experimental parameters and the quantum yields of HCHO formation measured after 0.5 Hz illumination of the oxygenated sample solutions by 200 laser pulses (10−20 ns pulse width). In the presence of neat colloidal TiO_2, ϕ_{HCHO} was 0.032 ± 0.002, ca. 50% larger than for CW photolysis. Likewise, ϕ_{HCHO} was increased by a factor of ca. 1.5 when the laser-pulse photolysis was applied on suspensions containing the platinized photocatalysts (1 wt % Pt), irrespective of the method of their preparation. Most importantly, it was found that repetitive laser-pulse photolysis improved ϕ_{HCHO} (Table 1) substantially and by the same factor (ca. 1.5) over CW photocatalysis (Figure 6) for all the photocatalysts studied although in both modes of photolysis the time-averaged molar photon absorption rate was approximately the same (ca. 8×10^{-7} einstein L^{-1} s^{-1}).

In all the photolyses described above the suspensions were saturated with oxygen. It was of interest to study the same systems in the absence of oxygen in order to determine the role of hydrogen ions as potential electron acceptors at pH 3.5. The effect of deoxygenation on ϕ_{HCHO} is documented in Table 2. Listed are the values of ϕ_{HCHO} in oxygen-free (i.e., nitrogen-saturated) suspensions containing 0.25 M CH_3OH and a loading of 0.1 g/L for all three photocatalysts. It should be noted that the concentration of CH_3OH and the number of laser pulses applied were larger in oxygen-free than in oxygen-saturated suspensions (Table 1). However, the number of e^-/h^+ pairs produced per photocatalyst particle per pulse was of the same order (0.3 ± 0.1) as was the time-averaged photon absorption rate. The pH was 3.5 throughout in laser-pulse and CW photolyses. As seen from Table 2, HCHO was produced with similar quantum yields compared with those measured in the presence of oxygen (Table 1). This indicates that a (photo)-electron acceptor other than O_2 is operative. However, a closer inspection of ϕ_{HCHO} in Tables 1 and 2 shows that neat TiO_2 and PtTi-S2 are less efficient photocatalysts for methanol oxidation in O_2-free than in O_2-saturated suspension, while the activity of PtTi-S1 remains virtually unchanged. A rationalization of these findings will be presented in the Discussion.

A summary of the quantum yields of HCHO formation by photocatalytic methanol oxidation measured under CW and repetitive laser-pulse illumination is given in Table 3.

4. Discussion

4.1. Optical Absorption. The UV−vis absorption spectra of the colloidal TiO_2-based photocatalysts (Figure 2) demonstrate that the presence of platinum does not influence the absorbance of neat colloidal TiO_2 in case of PtTi-S1 and has only a small effect in case of PtTi-S2. By use of the procedure proposed by Kormann et al.,[33] the band gap energy, E_g, of the colloidal TiO_2 sample can be derived from the data shown in Figure 2 as 3.35 eV, corresponding to an absorption onset at 370 nm. In comparison with bulk anatase TiO_2 ($E_g = 3.23$ eV[39]), the band gap of the neat colloidal TiO_2 particles (3.35 eV) is increased by 0.12 eV. The "particle-in-a-box" model given by Brus[40] suggests that the increased band gap energy arises from size quantization.

4.2. Network Structure. The TEM images (Figure 3) of the three TiO_2-based photocatalysts reveal aggregation of the particles and the formation of networks of different architectures. Aggregation of colloids is a well-known phenomenon usually explained by various particle−particle interaction potentials such as those used in the theory by Derjaguin, Landau, Verwey, and Overbeek (DLVO theory).[41,42] Adhesion in nanoscale systems is also an important issue in many other fields.[43]

As demonstrated by Figure 3, the particles in the platinized ($Pt@TiO_2$) samples PtTi-S1 and PtTi-S2 form much larger networks by apparently stronger aggregation than the particles in neat TiO_2. We offer the following tentative explanation for this striking difference. When considering materials on the near-atomic level, a number of forces exist between two surfaces as they approach each other. Colloidal particles such as those studied here are metastable. Their stability depends heavily on the attractive and repulsive interactions between them which are mainly controlled by the balance between van der Waals attraction and repulsive electrostatic potentials.[41,42] The TiO_2 particles prepared here under acidic conditions (section 2.2) carry a positive charge from protonated surface hydroxyl groups which is compensated by the negative charge of the mobile counteranions in the suspension.[10] Upon deposition of Pt clusters (PtTi-S1) or mixing with Pt nanoparticles (PtTi-S2) the surface charge on TiO_2 is lessened. Hence, there is no electrical field on those parts of the particle surface which are covered by Pt clusters or which are in contact with Pt particles. Therefore, the TiO_2 particles in $Pt@TiO_2$ are more apt to form aggregates than the neat ones (see Figures 3 and 4). Another consequence is that the spherical symmetry of the electrical field around a positively charged neat TiO_2 particle is lowered when parts of the surface are shielded by an electroneutral material. This may explain why the neat TiO_2 particles tend to form aggregates with no preferred orientation, quite different from the extended network structure of the particles in $Pt@TiO_2$ which consists of interconnected chainlike portions (Figure 3).

Aggregation to form network structures is of universal significance in colloid chemistry. In our previous work, three-dimensional networks of Fe(III)-doped TiO_2 nanoparticles/clusters[18,19] and of neat 2.4 nm TiO_2 particles[44] existing in

TABLE 1: Conditions and Quantum Yields of HCHO Formation in the Presence of TiO_2-Based Photocatalysts in O_2-Saturated Aqueous Methanol after Repetitive (0.5 Hz) Laser-Pulse Photolysis (XeF, 351 nm)[a]

	photocatalyst		
parameter	neat TiO_2 (2.4 nm)	PtTi-S1[c] (1.5−4.0 nm)	PtTi-S2[c] (1.5−4.0 nm)
catalyst loading/g L^{-1}	0.1	0.1	0.1
particle concentration/μmol L^{-1}	4.7	ca. 4.7	ca. 4.7
absorbance, A (351 nm)	0.10	0.11	0.12
absorption fraction, F_s, eqs 3 and 4	0.20	0.22	0.24
number, N, of laser pulses applied	200	200	200
incident photons, I_0, per pulse/einstein $\times 10^9$	6.37	7.84	5.08
photons absorbed by TiO_2 per pulse/μeinstein L^{-1}	1.45	2.03	1.43
number of e^-/h^+ pairs produced per particle per pulse	0.31	0.43	0.30
concentration of HCHO, C_{HCHO}/μmol L^{-1} after 200 pulses	2.58	5.39	3.94
quantum yield of HCHO, ϕ_{HCHO} [b]	0.032	0.047	0.048

[a] 30 mM methanol. For details see section 2.4. [b] $\phi_{HCHO} = C_{HCHO}V_R/(F_sI_0N)$; total volume of reaction solution, $V_R = 3$ mL. Note that the photolysis volume as controlled by the aperture (0.6 cm diameter), Scheme 1, was 0.85 mL. [c] Content of Pt, 1 wt %.

TABLE 2: Quantum Yields of HCHO Formation in the Presence of TiO_2-Based Photocatalysts in O_2-free (N_2-Saturated) Aqueous Methanol after Repetitive (0.5 Hz) Laser-Pulse Photolysis (XeF, 351 nm)[a]

	photocatalyst		
parameter	neat TiO_2 (2.4 nm)	PtTi-S1[c] (1.5−4.0 nm)	PtTi-S2[c] (1.5−4.0 nm)
catalyst loading/g L^{-1}	0.1	0.1	0.1
particle concentration/μmol L^{-1}	4.7	ca. 4.7	ca. 4.7
absorbance, A (351 nm)	0.10	0.11	0.12
absorption fraction, F_s, eqs 3 and 4	0.20	0.22	0.24
number, N, of laser pulses applied	690	600	600
incident photons, I_0, per pulse/einstein $\times 10^9$	6.59	5.30	4.04
photons absorbed by TiO_2 per pulse/μeinstein L^{-1}	1.55	1.37	1.14
number of e^-/h^+ pairs produced per particle per pulse	0.33	0.33	0.22
concentration of HCHO, C_{HCHO}/μmol L^{-1} after N pulses	8.15	11.48	6.47
quantum yield of HCHO, ϕ_{HCHO}[b]	0.027	0.049	0.033

[a] 0.25 M methanol, see also section 2.4. [b] See footnote b in Table 1. [c] Content of Pt 1 wt %.

TABLE 3: Summary of Quantum Yields, ϕ_{HCHO}, of Formaldehyde Formation from Aqueous Methanol at Various Nanocrystalline TiO_2-Based Photocatalysts under Different Conditions[a]

photocatalyst	CW photolysis 300−400 nm, O_2-saturated[b]	laser (XeF) pulse photolysis 351 nm, O_2-saturated[c]	laser (XeF) pulse photolysis 351 nm, N_2-saturated[d]
2.4 nm TiO_2	0.020 ± 0.001	0.032 ± 0.002	0.027 ± 0.002
1.5−4 nm PtTi-S1 (1 wt % Pt)	0.034 ± 0.003	0.047 ± 0.002	0.049 ± 0.002
1.5−4 nm PtTi-S2 (1 wt % Pt)	0.031 ± 0.002	0.048 ± 0.002	0.033 ± 0.002

[a] Catalyst loading 0.1 g L^{-1}, pH 3.5 and room temperature throughout. [b] $I_a = 8 \times 10^{-7}$ einstein L^{-1} s^{-1}, 30 mM methanol, Figure 6. [c] Train of 200 pulses (10−20 ns), repetition frequency 0.5 Hz, ca. 6×10^{-9} einstein/pulse (ca. 0.35 e^-/h^+ pairs per particle per pulse), $\langle I_a\rangle \cong 7-10 \times 10^{-7}$ einstein L^{-1} s^{-1} (time-average), 30 mM methanol, Table 1. [d] Train of 600−690 pulses (10−20 ns, 0.5 Hz), ca. 5×10^{-9} einstein/pulse (ca. 0.3 e^-/h^+ pairs per particle per pulse), $\langle I_a\rangle \cong 6-8\times 10^{-7}$ einstein L^{-1} s^{-1} (time-average), 250 mM methanol, Table 2.

solution have been observed directly by means of cryo-TEM. Similar aggregates of these particles in the dry state have been seen in TEM as well. This close resemblance suggests that aggregates and networks similar to those shown in Figure 3 are also present in the aqueous suspensions of the photocatalysts studied here. For such a network structure, a novel energy transfer mechanism has been proposed.[18,19] Implications of this aggregate/network structure for the photocatalytic activity of the TiO_2 and Pt@TiO_2 samples investigated here under CW and repetitive laser-pulse illumination (Table 3) will be discussed in sections 4.4 and 4.5.

4.3. Effect of Deoxygenation and Mechanisms of Formaldehyde Formation. Before discussing the mechanisms given in Scheme 2 it should be emphasized that, under the present experimental conditions, formaldehyde (HCHO) can be considered as a stable product of methanol oxidation not being further oxidized to formate or CO_2 and H_2O. Only a few micromoles of HCHO were formed (at most) in all the photolyses (cf. Figure 5 and Tables 1 and 2). Because of the competing oxidation of methanol present in large excess (0.03−0.25 M) over formaldehyde, the latter survives as a persistent intermediate during the time span of photolysis (≤50 min).

The present conditions of photolysis are close to those chosen by Sun and Bolton who determined the quantum yield of formaldehyde formation, ϕ_{HCHO}, from oxygenated aqueous methanol on TiO_2 (anatase) particulates in order to derive the quantum yield of the ·OH intermediate.[14] Scheme 2a summarizes the mechanism of photocatalytic HCHO formation in the presence of O_2 as proposed by Sun and Bolton.[14] In the first oxidation reaction, step 7, the $\cdot CH_2OH$ intermediate is formed from CH_3OH rapidly (either by ·OH attack or by a surface-trapped photohole). $\cdot CH_2OH$ is then further oxidized by O_2 to give HCHO. Reduction of O_2 by photogenerated electrons, step 6, has been assumed to be rate-controlling for the net reaction.[14] Hence, the rate of step 6 also controls ϕ_{HCHO}. This, in turn, is reflected by the decrease of ϕ_{HCHO} with

SCHEME 2: Mechanism of TiO_2-Photocatalyzed HCHO in the Presence of O_2 Saturation (a) and via Current-Doubling (b) in the Presence of e^- acceptor A (H^+ and/or Residual O_2) in N_2-Purged Suspension

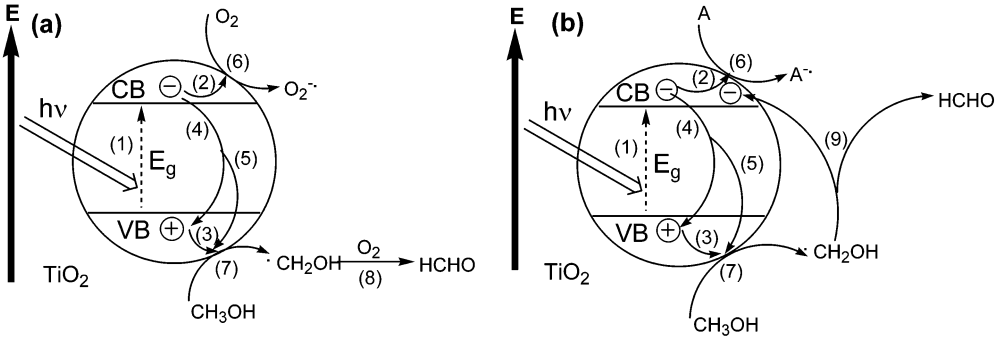

(1) Photogeneration of the charge carriers e^- and h^+; (2) and (3) surface trapping of the charge carriers; (4) and (5) recombination channels; (6) e^- transfer to the acceptor; formation of $O_2^{-\bullet}/HO_2^\bullet$ (a) or $A^{-\bullet}$ (b); (7) first oxidation step of CH_3OH; (8) formation of HCHO by e^- transfer from $\cdot CH_2OH$ to O_2; (9) formation of HCHO by e^- injection from $\cdot CH_2OH$ into the conduction band of TiO_2 (current-doubling).

increasing photon flux.[14−16] It should be noted that the mode of generation of $\cdot CH_2OH$ is not relevant for the discussion of the effects of deoxygenation and platinization observed in the present study. Further, $HO_2^\bullet$ ($pK_a = 4.8$[45]) rather than $O_2^{-\bullet}$ is the one-electron reduction product of O_2 at the pH of 3.5 used here.

In general, the presence of O_2 is considered as a prerequisite for efficient TiO_2-photocatalyzed oxidation of organic pollutants in wet systems.[46] Similarly, the gas-phase photocatalytic oxidation of 2-propanol to produce acetone and water on single-crystalline TiO_2 proceeds only in the presence of coadsorbed O_2.[47,48] Contrary to expectation, removal of O_2 by purging the suspensions with N_2 resulted in only a small decrease of ϕ_{HCHO} (ca. 15%) for neat TiO_2 and no change for PtTi-S1. A somewhat larger decrease of ϕ_{HCHO} (ca. 30%) was observed for PtTi-S2, see Table 3 (laser-pulse photolysis). Although O_2 may not have been removed completely by purging with N_2, the result suggests that in (nearly) oxygen-free suspensions a species A other than O_2 acts as photoelectron acceptor, and the $\cdot CH_2OH$ intermediate is converted to HCHO via a different route. This is illustrated in Scheme 2b.

In O_2-free suspensions of TiO_2 particles the photogenerated electron can be trapped by Ti^{IV} as an acceptor yielding a Ti^{III} center (the "trapped electron", e_{tr}^-) which has previously been characterized by time-resolved optical absorption spectroscopy in laser-flashed suspensions of the present[49] and of similar[21] TiO_2 particles

$$e^-_{photo} + Ti^{IV}(TiO_2) \rightarrow Ti^{III}(TiO_2) \qquad (5)$$

The e_{tr}^- state is long-lived (> ca. 0.1 s) in O_2-free suspensions containing a hole scavenger such as an alcohol, however, short-lived in the presence of O_2.[21] In the photolyses carried out here in N_2-saturated suspensions, Ti^{III} may have been reconverted slowly[49] to Ti^{IV} by residual O_2 remaining adsorbed on the TiO_2 particles even after purging with N_2. Hence, trace amounts of adsorbed O_2 could act as the final e^- acceptor (A in Scheme 2b) even in N_2-purged suspensions.

The $\cdot CH_2OH$ intermediate formed via a hole-scavenging process, step 7, is obviously further oxidized to produce HCHO in N_2-purged suspensions as well (cf. ϕ_{HCHO} in Table 3). In O_2-saturated solution, HCHO production has been attributed to oxidation of $\cdot CH_2OH$ by O_2 (Scheme 2a).[14] In the absence of O_2, the only way to form HCHO from $\cdot CH_2OH$ is via electron injection into the conduction band of TiO_2, see step 9 in Scheme 2b. This dark process is referred to as "current-doubling" in photoelectrochemistry and has been observed in many related

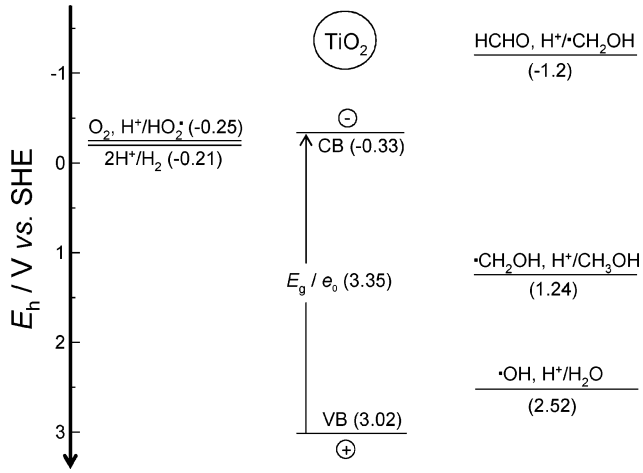

Figure 7. Formal standard potentials at pH 3.5 of redox couples relevant for the mechanisms of HCHO formation from methanol on illuminated neat TiO_2 particles (Scheme 2). Value for $\cdot CH_2OH$, H^+/CH_3OH calculated from thermodynamical data. Other one-electron reduction potentials taken from refs 55 and 56. E_{CB} of the TiO_2 particles adopted from ref 57. E_g derived from the present work (section 4.1.)

systems including the photoanodic oxidation of alcohols on TiO_2 electrodes.[50−54] From the diagram (Figure 7) of the formal standard potentials of the redox couples involved in the present photocatalytic system it is seen that e^- injection from $\cdot CH_2OH$ is thermodynamically allowed and is expected to proceed also in competition with oxidation of $\cdot CH_2OH$ by O_2. (We cannot differentiate between these two pathways of consumption of $\cdot CH_2OH$ because we were unable to measure the instantaneous quantum yield of $HO_2\cdot$.)

Another potential e^- acceptor in the absence of oxygen is the hydrogen ion ($A = H^+_{aq}$ and/or H^+_{ad} in Scheme 2b) present in the suspensions at pH 3.5. Reduction of H^+ to give H_2

$$2e^-_{CB/tr} + 2H^+_{aq/ad} \xrightarrow[dark]{} H_2 \qquad (6)$$

requires the transfer, on the same TiO_2 particle, of two electrons from the conduction band or e_{tr}^- state which is ca. 30 mV[58,59] below the conduction band. The two-electron requirement is met even after the absorption of just a single photon in case of current-doubling (Scheme 2b). Reaction 6 is thermodynamically allowed even at unity partial pressure of H_2 (Figure 7), since the potential of conduction-band electrons in TiO_2 particles is -0.12 ± 0.02 V versus the hydrogen electrode at the same pH.[57] In fact, H_2 evolution has been observed upon UV illumination of a deoxygenated TiO_2 sol at pH 3.[57]

For H^+ as the e^- acceptor, the rate of reaction 6 is expected to control ϕ_{HCHO} in the deoxygenated photolyte (Table 3). Reaction 6 is most likely hindered kinetically on neat TiO_2 particles, a property common to most oxide-type semiconductors in cathodic e^- transfer reactions.[60] On the other hand, H_2 formed under the present conditions would have a partial pressure, p_{H_2}, several orders of magnitude smaller than the standard pressure assumed for reversible $H_2/2H^+_{aq}$ potential (ca. -0.12 V vs E_{CB}) given in Figure 7. The strong decrease of p_{H_2} would shift the $H_2/2H^+_{aq}$ potential in the positive direction and, thus, supply a cathodic overvoltage much larger than -0.12 V and sufficient for compensating the kinetic hindrance of reaction 6. This may explain why ϕ_{HCHO} on neat TiO_2 particles was only slightly smaller in deoxygenated than in oxygenated suspension (Table 3, laser-pulse photolysis). Unfortunately, we were not able to measure ϕ_{H_2} in order to check the correlation with ϕ_{HCHO} expected for H^+ being the only e^- acceptor under our present conditions.

Finally, it should be noted that the net reaction pertaining to $A = H^+_{aq}$ (Scheme 2b)

$$CH_3OH_{aq} \rightarrow HCHO_{aq} + H_{2(g)} \qquad (7)$$

is endergonic ($\Delta G^\circ_{11} = +44.8$ kJ/mol).[55] The net reaction in case of $A = O_{2(aq)}$ (Scheme 2a)

$$2CH_3OH_{aq} + O_{2(aq)} \rightarrow 2HCHO_{aq} + 2H_2O_l \qquad (8)$$

is exergonic ($\Delta G^\circ_{12} = -208.7$ kJ/mol).[55] The values of ΔG° show that reaction 7 is photosynthetic, while reaction 8 is photocatalytic on illuminated TiO_2. $H_{2(g)}$ would be the stable product of reaction 7 in repetitive laser-pulse photolysis, if $H_{2(ad)}$ formed on the particles desorbs during the dark period between two laser pulses (2 s, cf. Table 2). H_2O_l in reaction 8 originates from disproportionation of the first-formed radical anion, $O_2^{-\cdot}$ (Scheme 2a), which protonates at pH 3.5.[45]

4.4. Platinization. Loading the TiO_2 surface with a small amount of Pt clusters or forming a contact between colloidal Pt and TiO_2 particles creates a sink for electrons, which facilitates the separation of e^-/h^+ pairs photogenerated in TiO_2.[61] Consequently, platinization decreases the recombination probability of photoholes with their counterparts (e^-_{CB} or e^-_{tr}) and increases the fraction of photoholes undergoing the oxidizing interfacial charge-transfer reaction. This has been demonstrated previously by time-resolved optical absorption spectroscopy in laser-pulsed suspensions of the TiO_2 particles used here.[49] As observed in the present work, the direct result of platinization is a substantial enhancement of the quantum yield of HCHO formation under all conditions of photolysis (Table 3).

Platinization has been achieved either by photodeposition (PtTi-S1) or by mixing of colloidal Pt and TiO_2 (PtTi-S2), see section 2.2. The former material appears to be more efficient than the latter for photocatalytic oxidation of CH_3OH to produce HCHO (cf. Figure 6 and Table 3). This can be explained in terms of differences in the electronic interaction between the metal and the TiO_2 support, in metal dispersity and in the mechanism of reduction of the electron acceptor (see section 4.3 and the discussion below).

The shape of the Pt component in PtTi-S1 and PtTi-S2 differs according to the preparation method and so does the extent of interaction between Pt and TiO_2. This apparently results in different promotion effects. Photodeposition of metals on TiO_2 has been studied extensively. Wang et al. investigated the deposition of Au from $AuCl_4^-$ on illuminated TiO_2 by means of TEM, HRTEM and XPS.[62,63] Well-defined Au clusters formed on the particle surface by the growth of Au nuclei were identified. Similarly, the analogous preparation of PtTi-S1 by photodeposition of Pt from $PtCl_6^{2-}$ should yield Pt clusters on the TiO_2 surface. In PtTi-S2 prepared by mixing of colloidal Pt with excess colloidal TiO_2, the Pt particles should rather be surrounded by TiO_2 particles. A corresponding proposal for the structure of the Pt promotion centers in the two photocatalysts is given in Scheme 3. The promotion centers are thought to be embedded in the chainlike structures of the particle aggregates seen in the TEM images of PtTi-S1 and PtTi-S2 (Figure 3).

SCHEME 3: Models of PtTi-S1 Formed by Photodeposition of Pt (a) and of PtTi-S2 Formed by Mixing of Colloidal Pt and TiO_2 (b)

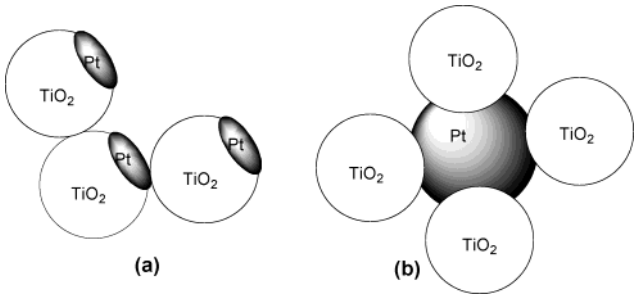

The Pt-atom/TiO_2-particle ratio for PtTi-S1 containing 1 wt % Pt is ca. 1:1. The formation of Pt clusters implies that only a fraction of the TiO_2 particles are platinized, e.g., 5% assuming uniform clusters containing 20 Pt atoms. The in situ growth of Pt clusters during photodeposition leaves little doubt that the electronic interaction between Pt and TiO_2 in PtTi-S1 is stronger than in PtTi-S2. This may explain why PtTi-S1 exhibits a stronger promotion effect than PtTi-S2 under some specific conditions. The effect is apparent during the CW photolysis in the presence of O_2 (Figure 6) and upon repetitive laser-pulse photolysis in the absence of O_2 (Table 3).

Component analysis[64] of PtTi-S2 (1 wt% Pt) gives a ca. 1:1060 molar ratio of Pt/TiO_2 nanoparticles. It is surprising to find that such a small fraction of Pt particles in PtTi-S2 increases ϕ_{HCHO} by ca. 50% in case of CW and laser-pulse illumination of the oxygenated photolytes, which is a substantial improvement over the yield measured in the presence of neat TiO_2 particles (Table 3). The observed enhancement of ϕ_{HCHO} cannot be explained solely by the action of highly photoactive Pt/TiO_2-particle complexes even if it is assumed that one Pt particle is in direct contact with 12 TiO_2 particles (i.e., the maximal numbers of nearest neighbors in a close-packed structure of uniform spheres) and that the quantum yield of HCHO formation is unity for such a complex. We therefore offer a modified explanation on the basis of our previously proposed "antenna effect" in networks of TiO_2 nanoparticles.[18] The principle of the mechanism is that an optically excited TiO_2 nanoparticle can transfer the absorbed energy (or the photogenerated charge carriers) through the network to another ground-state TiO_2 particle, whereby the probability of hole transfer to an adsorbed methanol molecule and the probability of electron transfer to the Pt particle are increased. In view of the chainlike particle aggregates seen in the TEM images of PtTi-S1 and PtTi-S2 (Figure 3) such a mechanism, which implies a large-range interaction between Pt centers and TiO_2 particles, may rationalize the surprisingly strong promotion effect by Pt.

Platinum as an electron sink on TiO_2 particles improves the photoactivity in general.[61] On the other hand, Pt apparently favors particle aggregation to form the chain structure (Figure 3) which is a prerequisite for the fast transport of excitation

energy or of photogenerated charge carriers postulated above. We believe that platinization, at least in the present case, has this dual function leading to the observed enhancement of ϕ_{HCHO} (Table 3).

Another interesting outcome of the present study is the dramatically different response of ϕ_{HCHO} to deoxygenation observed with PtTi-S1 and PtTi-S2 in laser-pulse photolysis (see the second and third column of Table 3). In contrast to PtTi-S2, ϕ_{HCHO} remains unchanged in the presence of PtTi-S1 when the suspension is purged with N_2. This points to different mechanisms of the photoelectron transfer to the acceptor at PtTi-S1 and PtTi-S2 in the absence of O_2.

The two platinized TiO_2 photocatalysts (abbreviated as Pt@TiO_2) were in contact with air during the preparation (section 2.2.). Under this condition Pt is partially covered with adsorbed OH groups.[65] Pt$-OH_{ad}$ is an efficient electrocatalyst for the reduction of O_2.[65,66] This and the action of Pt as an electron sink[61] explains why Pt@TiO_2 enhances ϕ_{HCHO} by about the same factor (ca. 1.5−1.7) in comparison with neat TiO_2 particles in the oxygenated suspension (Table 3). Apparently, the process

$$O_2 + e^- \xrightarrow[(Pt@TiO_2)]{Pt|Pt-OH_{ad}} O_2^{-\bullet} \xrightarrow{H^+} HO_2^{\bullet} \qquad (9)$$

catalyzed by Pt|Pt$-OH_{ad}$ on Pt@TiO_2 is rate-controlling for the formation of HCHO in the oxygenated suspension as previously suggested[14−16] for neat TiO_2.

In the absence of O_2, reaction 9 is replaced by photocathodic net reaction

$$2H^+ + 2e^- \xrightarrow[(Pt@TiO_2)]{} H_2 \qquad (10)$$

This has been shown previously by Bahnemann et al. who reported quantum yields of up to 0.045 for H_2 formation in illuminated aqueous suspension (pH 3) containing methanol and mixtures of colloidal Pt and TiO_2 particles.[61] These values of ϕ_{H_2} are close to the values of ϕ_{HCHO} determined here in the deoxygenated suspensions containing Pt@TiO_2 (Table 3). This is consistent with control of ϕ_{HCHO} by the rate of consumption of photoelectrons via reaction 10 after their transfer to the Pt component.

Reaction 10 is electrocatalyzed by Pt free of adsorbed OH groups.[65,66] For efficient catalysis, Pt$-OH_{ad}$ initially present on Pt@TiO_2 has to be reduced to give electroactive Pt. (This step consumes a small fraction of the photoelectrons generated by the 600 laser pulses applied for the production of HCHO, see Table 2.) Once the reduction of Pt$-OH_{ad}$ is completed, both PtTi-S1 and PtTi-S2 electrocatalyze the one-electron reduction of H^+ yielding H_{ad} on Pt[66]

$$H^+ + e^- \xrightarrow[(Pt@TiO_2)]{Pt} H_{ad} \qquad (11)$$

H_2 is then formed on Pt by one of the following reactions

$$H_{ad} + H_{ad} \xrightarrow[(Pt@TiO_2)]{Pt} H_2 \qquad (12)$$

or

$$H_{ad} + H^+ + e^- \xrightarrow[(Pt@TiO_2)]{Pt} H_2 \qquad (13)$$

where the current-doubling mechanism (Scheme 2b) assists in supplying the additional electron.

The rate of cathodic H_2 evolution at a given overvoltage depends on the dispersity of Pt. It is known that H_2 evolution via reactions 11 and 12 on platinized Pt is faster at the same overvoltage than via reactions 11 and 13 which proceed on bright platinum.[66] The same reaction is expected for the electrocatalysis of H_2 evolution on the two types of Pt@TiO_2. Finely dispersed Pt formed as a cluster on the TiO_2 particles in PtTi-S1 (Scheme 3a) should strongly catalyze the consecutive reactions 11 and 12, while the compact Pt particles in PtTi-S2 (Scheme 3b) should be the poorer electrocatalyst for H_2 evolution which in this case is expected to proceed via reactions 11 and 13. From these considerations and the assumption that the reduction of H^+ is rate-controlling for the formation of HCHO in O_2-free suspension, it can be understood why ϕ_{HCHO} on PtTi-S1 is found to be larger than on PtTi-S2, see the last row in Table 3. It should be noted that size and dispersity dependent effects in Pt-mediated electrocatalysis have also been reported by Cherstiouk et al.[67] and Savinova et al.[68]

4.5. Repetitive Laser-Pulse Illumination. Irrespective of the photocatalyst employed, repetitive laser-pulse illumination increased ϕ_{HCHO} in the oxygenated suspensions by a factor of ca. 1.5 in comparison with CW illumination, although in both modes of photolysis the time-averaged photon absorption rate was approximately the same (Table 3). Previous studies on intermittent illumination in TiO_2 photocatalysis[27−32] offer no explanation for this observation.

Cornu et al. investigated the quantum yield, ϕ_F, of photocatalytic formate oxidation in oxygenated acidic TiO_2 suspension under continuous and periodic pulse illumination.[32] They rationalized their results with reference to a mechanism which leads to

$$\phi_F = \beta\langle I_a\rangle^{n-1}, \quad 0.5 \le n \le 1 \qquad (14)$$

where β is a proportionality constant and $\langle I_a\rangle$ is the time-averaged photon absorption rate. Under continuous illumination, $(n-1)$ was determined as -0.39.[32] For very short illumination times in periodic pulse photolysis, Cornu et al. demonstrated that ϕ_F was identical to the value obtained under continuous illumination, eq 14, at the same time-averaged photon absorption rate. This is in sharp contrast to our results for photocatalytic methanol oxidation (Table 3).

Our mechanism of photocatalytic HCHO formation and our previous measurement of ϕ_{HCHO} under CW illumination at different photon absorption rates, I_a, in oxygenated aqueous methanol containing the present neat colloidal TiO_2 photocatalyst yielded[16]

$$\phi_{HCHO}(CW) \cong kI_a^{-1/2} \qquad (15)$$

which is analogous to the relation for ϕ_F, eq 14. Under the tacit assumption that laser flashing does not change the state of the present photocatalyst, the result by Cornu et al.[32] suggests that under repetitive laser-pulse illumination should be given by

$$\phi_{HCHO}(pulse) \cong k\langle I_a\rangle^{-1/2} \qquad (16)$$

From eqs 15 and 16 the expected ratio of the quantum yields is

$$\frac{\phi_{HCHO}(pulse)}{\phi_{HCHO}(CW)} \cong \left[\frac{\langle I_a\rangle(pulse)}{I_a(CW)}\right]^{-1/2} \qquad (17)$$

Taking $I_a = 8 \times 10^{-7}$ einstein L^{-1} s^{-1} and $\langle I_a\rangle \cong 8.5 \times 10^{-7}$ einstein L^{-1} s^{-1} (Table 3) applied in CW and repetitive laser-pulse photolysis, respectively, the expected value of ϕ_{HCHO}-

SCHEME 4: Laser-Pulse-Induced Deaggregation of a Close-Packed TiO_2-Particle Tetramer Resulting in Single Particles with Additional Sites for Reactant Adsorption

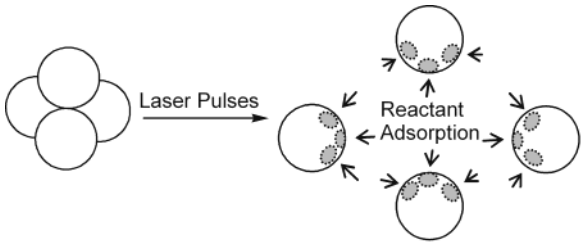

(pulse)/ϕ_{HCHO}(CW), 0.97, is significantly smaller than the value, 1.6 ± 0.2, measured in the presence of neat colloidal TiO_2. The same conclusion holds for the measurements employing Pt@TiO_2 (Table 3).

As a tentative explanation of the increase of ϕ_{HCHO} obtained by repetitive laser-pulse illumination we propose laser-pulse stimulated deaggregation of the TiO_2-particle agglomerates shown in the TEM images (Figures 3 and 4). Such a process would increase the surface area available for reactant adsorption at a given photocatalyst loading and would thus lead to an increase of the photocatalytic reaction rate, and of ϕ_{HCHO}, upon applying a large number of laser pulses at a given average photon absorption rate. (This concept has been used for the interpretation of data obtained by laser-induced optoacoustic calorimetry of suspensions of the neat colloidal TiO_2 photocatalyst in the presence of halide ions. Unexpected exothermal effects could be understood by halide adsorption on sites set free by laser-pulse stimulated TiO_2-particle deaggregation.[69])

The TEM images (Figures 3 and 4) show relatively small but compact aggregates of single particles. Scheme 4 illustrates the deaggregation of a close-packed tetramer of TiO_2 particles as an example. Additional reactant adsorption takes place on portions of the single-particle surface initially shielded in the aggregate. For a rough estimate of the photocatalyst surface by deaggregation we assume that $^1/_{12}$ of the single-particle surface is shielded from adsorption by the presence of one adjacent particle. (A spherical particle inside a close-packed structure of identical spheres is surrounded by 12 nearest neighbors and would not contribute to adsorption.) From the comparison of the surface of the four single particles, 4*A*, in Scheme 4 with the unshielded surface of the tetramer, $4A - (^{12}/_{12})A$, the catalyst surface available for adsorption increases by a factor of 1.33 upon deaggregation. For a pentamer formed by the attachment of another particle to the tetramer the corresponding factor is 1.43. The factor increases with the number of particles in a close-packed aggregate.

From the TEM images (Figures 3 and 4) neither the configuration nor the size distribution of the aggregates in neat colloidal TiO_2 can be inferred precisely. Further, the particles are polyhedra rather than spheres. Nevertheless, the estimates of the increase of the photocatalyst surface given above substantiate the assumption that photostimulated deaggregation in repetitive laser-pulse photolysis is a plausible model to explain the 1.6-fold increase of ϕ_{HCHO} in the presence of neat colloidal TiO_2. The energetic requirement for deaggregation is met. The average number of photons absorbed per TiO_2 particle per laser pulse is 0.3 (Table 1). The average photon energy deposited in the particle tetramer (Scheme 4) is therefore at least 341 kJ mol^{-1} per laser pulse at 351 nm. The interparticle bond energy is only ca. 30 kJ mol^{-1}.[69] The photocatalytic formation of HCHO from $CH_3OH + O_2$ is exothermal. The energy supplied by the first few of the 200 pulses applied for photolysis (Table 1) would therefore be sufficient for the supposedly stepwise deaggregation of even larger agglomerates than the tetramer. Reaggregation of the particles is a slow process. This is concluded from the temporal evolution of small UV spectral changes observed after suspending the neat TiO_2 colloid and from a kinetic study[70] of reversible agglomeration of TiO_2 nanocolloids. Diffusion of reactants is not rate controlling under the conditions of this and related studies of photocatalytic processes.[32]

In CW photolysis the absorption of a photon is a rare event compared with the high-intensity illumination by the laser pulse. The aggregation remains intact under CW illumination because there is enough time for redistribution of the photon energy among the many vibrational modes before the same aggregate absorbs a second photon.

In the presence of PtTi-S1 and PtTi-S2, ϕ_{HCHO}(pulse)/ϕ_{HCHO}(CW) was 1.4 ± 0.2 and 1.6 ± 0.2, respectively, comparable to the result for neat colloidal TiO_2. The strong promotional effect on ϕ_{HCHO} by Pt was retained under repetitive laser-pulse illumination (Table 3). In principle, the findings can be rationalized by laser-pulse stimulated fragmentation of the large networks composed of very many aggregated particles in Pt@TiO_2 (Figure 3). However, in addition it must be assumed that the photofragments contain enough platinized TiO_2 particles (PtTi-S1) or Pt particles (PtTi-S2) to preserve the promotion of photocatalytic HCHO formation.

5. Conclusions

Quantum yields, ϕ_{HCHO}, of formaldehyde formation from methanol in oxygenated aqueous suspensions of colloidal TiO_2-based photocatalysts have been determined. Platinization of colloidal TiO_2 (ca. 2.4 nm particle size) by photodeposition (PtTi-S1) and by mixing with colloidal Pt (PtTi-S2) increases ϕ_{HCHO} under CW illumination by 70% and 50%, respectively, at a Pt content of 1 wt % which corresponds to a Pt/TiO_2 particle ratio of only ca. 1:1060 in PtTi-S2. TEM reveals particle aggregates in colloidal TiO_2 and extended networks of agglomerated particles in PtTi-S1 and PtTi-S2. It is concluded that the network structure has to be taken into account for the understanding of the strong enhancement of ϕ_{HCHO} by such a small amount of Pt. Transfer of excitation energy or of photogenerated charge carriers through the network is suggested to explain the increased quantum yields of methanol oxidation observed for the platinized TiO_2 particles. Under repetitive laser-pulse illumination ϕ_{HCHO} is increased by ca. 50% for all the photocatalysts in comparison with CW illumination at the same average photon absorption rate. This unexpected observation is tentatively explained by an increase of the photocatalyst surface caused by laser-pulse stimulated deaggregation of colloidal TiO_2 and by fragmentation of the networks in case of the platinized samples. In deoxygenated suspensions at pH 3.5 ϕ_{HCHO} is apparently controlled by the rate of H_2 formation. Pt as an electron sink and an electrocatalyst for H_2 evolution enhances ϕ_{HCHO}. The larger photoactivity of PtTi-S1 in this process is attributed to the high dispersity of Pt formed by photochemical deposition. All the observations suggest that structural properties of the photocatalysts such as aggregation/deaggregation and Pt-assisted network formation as well as the dispersity of Pt contribute to the photoactivity under the specific experimental conditions applied for methanol oxidation. Further studies concerning the response of the structural features to the illumination parameters are needed.

Acknowledgment. Chuan-yi Wang thanks the Alexander von Humboldt (AvH) foundation for a Research Fellowship

Grant. The authors thank Dr. Christoph Böttcher, Freie Universität Berlin, Forschungszentrum für Elektronenmikroskopie, for taking the electron micrographs. The authors also thank Mr. Thomas Kolrep, Freie Universität Berlin, Institut für Chemie, for his assistance in HPLC measurements. Financial support from the Deutsche Forschungsgemeinschaft (Grants BA 1137/3-1, BA 1137/4-1, and DO 150/7-1) is gratefully acknowledged.

References and Notes

(1) Serpone, N.; Pelizzetti, E. *Photocatalysis: Fundamentals and Applications*; Wiley: New York, 1989.

(2) *Photochemical Conversion and Storage of Solar Energy*; Pelizzetti, E., Schiavello, M., Eds.; Kluwer Academic Publishers: The Netherlands, 1991, and references therein.

(3) Fox, M. A.; Dulay, M. T. *Chem. Rev.* **1993**, *93*, 341−357.

(4) Kamat, P. V. *Chem. Rev.* **1993**, *93*, 267−300.

(5) Mills, A.; Davies, R. H.; Worsley, D. *Chem. Soc. Rev.* **1993**, *22*, 417−425.

(6) *Photocatalytic Purification and Treatment of Water and Air*; Ollis, D. F., Al-Ekabi, H., Eds; Elsevier: 1993.

(7) Bahnemann, D. W.; Cunningham, J.; Fox, M. A.; Pelizzetti, E.; Pichat, P.; Serpone, N. In *Aquatic and Surface Photochemistry*; Helz, G. R., Zepp, R. G., Crosby, D. G., Eds.; Lewis Publishers: Boca Raton, FL, 1994.

(8) Pichat, P. *Catal. Today* **1994**, *19*, 313−333.

(9) Heller, A. *Acc. Chem. Res.* **1995**, *28*, 503−508.

(10) Hoffmann, M. R.; Martin, S. T.; Choi, W. Y.; Bahnemann, D. W. *Chem. Rev.* **1995**, *95*, 69−96.

(11) Bahnemann, D. W. *Environmental Photochemistry*; Boule, P., Ed.; Springer: Berlin, New York, 1999.

(12) Fujishima, A.; Hashimoto, K.; Watanabe, T. *TiO_2 Photocatalysis: Fundamentals and Applications*; BKC: Tokyo, Japan, 1999.

(13) Bahnemann, D., Cassano, A. E., Eds. *Special Issue on TiO_2 Photocatalytic Purification and Treatment of Water and Air*; Science & Technology Network Inc.: London, Ontario, Canada, 2002.

(14) Sun, L. Z.; Bolton, J. R. *J. Phys. Chem.* **1996**, *100*, 4127−4134.

(15) Wang, C.; Bahnemann, D. W.; Dohrmann, J. K. *Water Sci. Technol.* **2001**, *44*, 279−286.

(16) Wang, C. Y.; Rabani, J.; Bahnemann, D. W.; Dohrmann, J. K. *J. Photochem. Photobiol., A* **2002**, *148*, 169−176.

(17) Wang, C. Y.; Bahnemann, D. W.; Dohrmann, J. K. *Chem. Commun.* **2000**, 1539−1540.

(18) Wang, C. Y.; Böttcher, C.; Bahnemann, D. W.; Dohrmann, J. K. *J. Mater. Chem.* **2003**, *13*, 2322−2329.

(19) Wang, C.-Y.; Böttcher, C.; Bahnemann, D. W.; Dohrmann, J. K. *J. Nanopart. Res.* **2004**, *6*, 119−122.

(20) Litter, M. I.; Navio, J. A. *J. Photochem. Photobiol., A* **1996**, *98*, 171−181.

(21) Bahnemann, D.; Henglein, A.; Lilie, J.; Spanhel, L. *J. Phys. Chem.* **1984**, *88*, 709−711.

(22) Izumi, I.; Fan, F.-R. F.; Bard, A. J. *J. Phys. Chem.* **1981**, *85*, 218−223.

(23) Uosaki, K.; Yoneda, R.; Kita, H. *J. Phys. Chem.* **1985**, *89*, 4042−4046.

(24) Nosaka, Y.; Kishimoto, M.; Nishino, J. *J. Phys. Chem. B* **1998**, *102*, 10279−10283.

(25) Vorontsov, A. V.; Stoyanova, I. V.; Kozlov, D. V.; Simagina, V. I.; Savinov, E. N. *J. Catal.* **2000**, *189*, 360−369.

(26) Kim, S.; Choi, W. *J. Phys. Chem. B* **2002**, *106*, 13311−13317.

(27) Sczechowski, J. G.; Koval, C. A.; Noble, R. D. *J. Photochem. Photobiol., A* **1993**, *74*, 273−278.

(28) Upadhya, S.; Ollis, D. F. *J. Phys. Chem. B* **1997**, *101*, 2625−2631.

(29) Buechler, K. J.; Nam, C. H.; Zawistowski, T. M.; Noble, R. D.; Koval, C. A. *Ind. Eng. Chem. Res.* **1999**, *38*, 1258−1263.

(30) Buechler, K. J.; Noble, R. D.; Koval, C. A.; Jacoby, W. A. *Ind. Eng. Chem. Res.* **1999**, *38*, 892−896.

(31) Buechler, K. J.; Zawistowski, T. M.; Noble, R. D.; Koval, C. A. *Ind. Eng. Chem. Res.* **2001**, *40*, 1097−1102.

(32) Cornu, C. J. G.; Colussi, A. J.; Hoffmann, M. R. *J. Phys. Chem. B* **2001**, *105*, 1351−1354.

(33) Kormann, C.; Bahnemann, D. W.; Hoffmann, M. R. *J. Phys. Chem.* **1988**, *92*, 5196−5201.

(34) Bockelmann, D.; Lindner, M.; Bahnemann, D. W. In *Fine Particles Science and Technology: From Micro to Nanoparticles*; Pelizzetti, E., Ed.; Kluwer Academic Publishers: Boston, Dordrecht, 1996.

(35) Heller, H. G.; Langan, J. R. *J. Chem. Soc., Perkin Trans. 2* **1981**, 341−343.

(36) Shriner, R. L. *The Systematic Identification of Organic Compounds: A Laboratory Manual*, 6th ed.; Wiley: New York, 1980.

(37) Potter, W.; Karst, U. *Anal. Chem.* **1996**, *68*, 3354−3358.

(38) Koivusalmi, E.; Haatainen, E.; Root, A. *Anal. Chem.* **1999**, *71*, 86−91.

(39) Goodenough, J. B.; Hammett, A. In *Landolt-Börnstein, New series, Group III*; Madelung, O., Ed.; Springer-Verlag: Berlin, Heidelberg, New York, Tokyo, 1984; Vol. 17g, p 147.

(40) Brus, L. *J. Phys. Chem.* **1986**, *90*, 2555−2560.

(41) Verwey, E. J. W.; Overbeek, J. T. G. *Theory of the Stability of Lyophobic Colloids; The Interaction of Sol Particles Having an Electric Double Layer*; New York Elsevier Pub. Co.: Amsterdam, 1948.

(42) Hiemenz, P. C. *Principles of Colloid and Surface Chemistry*, 2nd ed., revised and expanded; M. Dekker: New York, 1986.

(43) Rosoff, M. *Nano-surface Chemistry*; Marcel Dekker: New York, 2002.

(44) Pagel, R.; Böttcher, C. Unpublished results available upon request (E-mail: pagel@chemie.fu-berlin.de).

(45) Behar, D.; Czapski, G.; Rabani, J.; Dorfman, L. M.; Schwarz, H. A. *J. Phys. Chem.* **1970**, *74*, 3209−3213.

(46) Wang, C. Y.; Liu, C. Y.; Shen, T. *J. Photochem. Photobiol., A* **1997**, *109*, 65−70.

(47) Brinkley, D.; Engel, T. *Surf. Sci.* **1998**, *415*, L1001−L1006.

(48) Brinkley, D.; Engel, T. *J. Phys. Chem. B* **1998**, *102*, 7596−7605.

(49) Bahnemann, D. W.; Hilgendorff, M.; Memming, R. *J. Phys. Chem. B* **1997**, *101*, 4265−4275.

(50) Nosaka, Y.; Sasaki, H.; Norimatsu, K.; Miyama, H. *Chem. Phys. Lett.* **1984**, *105*, 456−458.

(51) Hykaway, N.; Sears, W. M.; Morisaki, H.; Morrison, S. R. *J. Phys. Chem.* **1986**, *90*, 6663−6667.

(52) Nogami, G.; Kennedy, J. H. *J. Electrochem. Soc.* **1989**, *136*, 2583−2588.

(53) Memming, R. In *Electron Transfer I*; Springer-Verlag: Berlin, New York, 1994; Vol. 169, pp 105−181.

(54) Memming, R. *Semiconductor Electrochemistry*; Wiley-VCH: New York, Weinheim, 2001.

(55) Bard, A. J., Parsons, R., Jordan, J., Eds. *Standard Potentials in Aqueous Solution*, 1st ed.; M. Dekker: New York, 1985.

(56) Wardman, P. *J. Phys. Chem. Ref. Data* **1989**, *18*, 1637.

(57) Duonghong, D.; Ramsden, J.; Grätzel, M. *J. Am. Chem. Soc.* **1982**, *104*, 2977−2985.

(58) Martin, S. T.; Herrmann, H.; Choi, W. Y.; Hoffmann, M. R. *J. Chem. Soc., Faraday Trans.* **1994**, *90*, 3315−3322.

(59) Martin, S. T.; Herrmann, H.; Hoffmann, M. R. *J. Chem. Soc., Faraday Trans.* **1994**, *90*, 3323−3330.

(60) Morrison, S. R. *Electrochemistry at Semiconductor and Oxidized Metal Electrodes*; Plenum Press: New York, 1980.

(61) Bahnemann, D.; Henglein, A.; Spanhel, L. *Faraday Discuss.* **1984**, 151−163.

(62) Wang, C. Y.; Liu, C. Y.; Zheng, X.; Chen, J.; Shen, T. *Colloid Surf., A* **1998**, *131*, 271−280.

(63) Wang, C. Y.; Liu, C. Y.; Chen, J.; Shen, T. *J. Colloid Interface Sci.* **1997**, *191*, 464−470.

(64) Assuming Pt nanoparticles are spherelike, the volume of one 3 nm Pt nanoparticles is 14.13 nm^3. Considering the mass density of platinum is 21.4 g cm^{-3}, the average weight of one Pt nanoparticle is derived as ca. 3.02×10^{-19} g. Likewise, the mass density of anatase TiO_2 is 3.894 g cm^{-3}, so the average weight of a 2.4 nm TiO_2 nanoparticle ($V \sim 7.23$ nm^3) is ca. 2.82×10^{-20} g. Therefore, the average weight ratio between Pt and TiO_2 nanoparticles is obtained: $W_{(Pt)n}/W_{(TiO2)m} \cong 10.7$, and the molar ratio of Pt/TiO_2 in PtTi-S2 (1 wt % Pt) is derived as ca. 1:1060.

(65) Woods, R. V. *Electroanal. Chem.* **1976**, *9*, 1−162.

(66) Vetter, K. J. *Electrochemical Kinetics: Theoretical and Experimental Aspects*; Academic Press: New York, 1967.

(67) Cherstiouk, O. V.; Simonov, P. A.; Chuvilin, A. L.; Savinova, E. R. *Proc. − Electrochem. Soc.* **2001**, *2000−20*, 56−71.

(68) Savinova, E. R.; Lebedeva, N. P.; Simonov, P. A.; Kryukova, G. N. *Russ. J. Electrochem. (Translation of Elektrokhimiya)* **2000**, *36*, 952−959.

(69) Pagel, R. Seminars given at the Institut fuer Technische Chemie, Universitaet Hannover, 2003. Material available upon request (E-mail: pagel@chemie.fu-berlin.de).

(70) Vorkapic, D.; Matsoukas, T. *J. Colloid Interface Sci.* **1999**, *214*, 283−291.